The Electronic Structure of Hydrogen Bonding in α-Oxalic Acid Dihydrate *

M. Weisser and W. Weyrich

Fakultät für Chemie, Universität Konstanz, D-W-7750 Konstanz, Fed. Rep. of Germany

Z. Naturforsch. **48a**, 315–324 (1993); received January 28, 1993

Compton spectra of α-oxalic acid dihydrate single-crystal slices and powder samples were measured in a helium atmosphere using 59.537 keV ^{241}Am radiation. In the anisotropic case, the scattering vector was oriented parallel to the shortest hydrogen bond, in the direction of the C = O bond, parallel to the C – O bond and perpendicular to the (*a*, *c*)-plane. The comparison of theoretical reciprocal form factors, calculated with a local density-approximation (LDA) method for an α-$(COOH)_2 \cdot 2H_2O$ cluster in triple-zeta basis-set quality, with the experimental data has demonstrated that there is a considerable influence of intermolecular interactions on the electronic structure. Further calculations including the intermolecular interactions of the first coordination sphere by symmetrical orthogonalisation of the LDA wave functions clearly improved the agreement of experiment and theory. A theoretical analysis of the reciprocal form factor $B^a(s)$ in the direction of the three different hydrogen bonds of α-oxalic acid dihydrate on the basis of the cluster calculations has shown that in the region above $s = 1.9$ Å all these bonds are dominated by electrostatic attraction and exchange repulsion of the donor and the acceptor system.

Key words: α-Oxalic acid dihydrate; Compton spectroscopy; Hydrogen bonding; Reciprocal form factor; Density functional calculations.

1. Introduction

Compton scattering is an interesting and useful method for studying intramolecular and intermolecular interactions such as hydrogen bonding in condensed matter [1]. The experiment uses X-ray or γ-ray photons, which excite the electrons of a target into unbound states by transferring energy and momentum in an inelastic scattering process. A Compton band results in the spectrum of scattered photons that, in the model of vertical transitions of a quasi-free electron gas (impulse approximation), reflects the distribution of momentum components $\boldsymbol{q}$ of the electrons of the sample in the direction of the scattering vector $\boldsymbol{k}$. The Compton profile $J(\boldsymbol{q})$ (experimentally convoluted with a resolution function $R(q)$ to $J^c(\boldsymbol{q})$) is the one-dimensional projection of the three-dimensional momentum density $\pi(\boldsymbol{p})$ onto the $\boldsymbol{k}$-vector (for reviews see, e.g., [2, 3]). In single-crystal measurements, it is dependent on the orientation of the scattering vector relative to the crystal coordinate system, thus enabling one to obtain detailed directional information on the chemical bonds and interactions in solid state.

At the IUCr conference in 1975, α-oxalic acid dihydrate, α-$(COOH)_2 \cdot 2H_2O$, was selected as an object for comparing best-possible experimental electron density maps from different laboratories, resulting in a great number of X-ray and neutron diffraction analyses [4]. With these experimental data [4, 5] and by comparison with structure factors based on refined vibrationally averaged theoretical electron density distributions, Krijn et al. [6, 7] demonstrated the influence of the shortest hydrogen bond and the crystal environment on the electron density in α-$(COOH)_2 \cdot 2H_2O$ and lowered the X-ray crystallographic R-factor from 1.3% to 1.0%.

Owing to the large number of types of chemical bonds in the crystal, the nearly (anti-)parallel orientation of these bonds and its low photoabsorption coefficient, α-oxalic acid dihydrate is also an interesting subject for Compton scattering and offers a particularly favourable opportunity to combine position and momentum-space data to a complete picture of the electronic structure. The reciprocal form factor $B^a(s)$, which is the final result of our data processing of α-$(COOH)_2 \cdot 2H_2O$ Compton spectra, contains information not present in the position density $\varrho(\boldsymbol{r})$ about

* Presented at the Sagamore X Conference on Charge, Spin and Momentum Densities, Konstanz, Fed. Rep. of Germany, September 1–7, 1991.

Reprint requests to Prof. Dr. Dr. h.c. Wolf Weyrich, Lehrstuhl für Physikalische Chemie I, Fakultät für Chemie, Universität Konstanz, Postfach 55 60, D-W-7750 Konstanz, Fed. Rep. of Germany.

0932-0784 / 93 / 0100-0315 $ 01.30/0. – Please order a reprint rather than making your own copy.

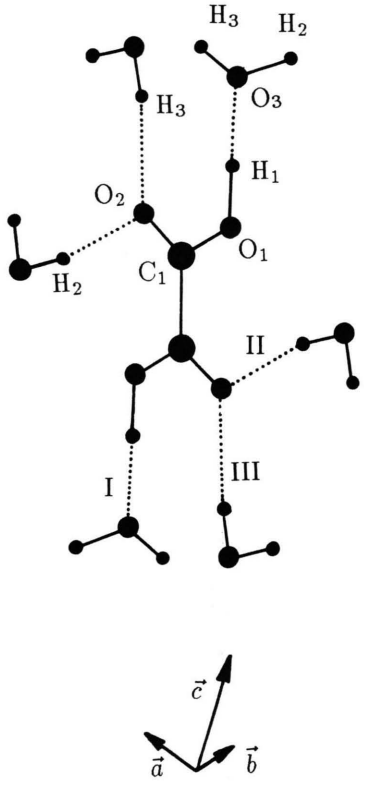

Fig. 1. The oxalic-acid molecule in crystalline α-$(COOH)_2 \cdot 2H_2O$ is surrounded by six nearest-neighbour H_2O molecules. The three different hydrogen bonds are marked by Roman numerals with increasing bond length.

the electronic structure of chemical bonding in the crystal environment. The corresponding theoretical $B^a(s)$ were calculated with the same basis set [7], crystal coordinates [5] and density functional that Krijn et al. [6] have used for their comparison of the electron density distributions. For this reason, the influence of the intermolecular interactions on the electron density and the reciprocal form factor can be compared without artefacts of different input parameters.

α-Oxalic acid dihydrate has a monoclinic structure (space group $P2_1/c$) that is built up of chains of oxalic-acid and water molecules connected by various hydrogen bonds. The oxalic-acid molecule is a donor of two short hydrogen bonds with a length [5] of 1.418 Å (I in Fig. 1) and an acceptor of four weak hydrogen bonds with lengths of 1.88 Å and 1.92 Å (II, III in Fig. 1), respectively.

Therefore, the theoretical calculations of $B^a(s)$ started from the assumption that the electronic structure of α-$(COOH)_2 \cdot 2H_2O$ can be described as a superposition of oxalic-acid and water wave functions. The intermolecular interactions were then introduced step by step by increasing the cluster size, thus making it possible to analyse the influence of the different bonding effects in the reciprocal form factor.

2. Experimental Details

The single crystals of α-$(COOH)_2 \cdot 2H_2O$ were obtained by growing seeds in a saturated aqueous solution or aceton-water mixture [8] in a temperature range of 40° to 28 °C with cooling rates of 0.025–0.050 °C per day. The orientation of the crystallographic $\boldsymbol{k}$-vector of the prepared thin crystal slices (thickness $d = 1.51$ mm–2.9 mm) was done with the Laue technique. The aim of our current single-crystal measurements is to obtain a great number of different directional reciprocal form factors to be used to reconstruct the three-dimensional momentum density of α-$(COOH)_2 \cdot 2H_2O$. The complete data set of these time-consuming anisotropic measurements (9 days per direction) will be the subject of a future publication.

The powder samples ($d = 0.75$ mm–4.61 mm, 7 samples) consisted of finely pulverised α-oxalic acid dihydrate, which were molded to thin slabs by pressure. The disk shape of the samples decreased the multiple-scattering error, which was additionally corrected by extrapolation to zero thickness [9]. The isotropic data are given in Table 1. The Compton measurements were carried out in a helium atmosphere in order to prevent the hydrate water from being quickly removed, which would be the case in vacuum [10]. The vapour pressure was kept constant with $CuSO_4 \cdot 5H_2O$ powder in the sample chamber. Manganometric titrations and weighing of the samples after the measurements guaranteed a purity of higher than 99.5%.

The ^{241}Am sources have an intense 59.537 keV γ-ray emission, which was employed as primary energy $\hbar\omega_1$. The scattering angle of the spectrometer was 159.6° for the single-crystal experiment and 165.1° for the powder experiment. The scattered radiation was analysed with a planar intrinsic Ge detector (Princeton-Gamma-Tech).

The Compton profiles $J^c(q)$ obtained from our data processing are at first convoluted with a Gaussian of full width at half maximum $\Delta q = 0.542\, p_0$ for the directional and $\Delta q = 0.604\, p_0$ for the isotropic measurements ($p_0 = \hbar/a_0 = 1$ Dumond $= 1.99289 \cdot 10^{-24}$

Table 1. The isotropic $B^a(s)$, experiment vs. theory. The σ of the experiment is between 0.0095 ($s = 2.1$ Å), 0.010 ($s = 3.15$ Å), 0.046 ($s = 1.05$ Å) and 0.075 ($s = 0.45$ Å). The momentum range for the Fourier analysis of the experimental Compton profils is $\pm 11.0831\ p_0$ ((b)–(f) analogous to Figure 3a).

s/Å	$B^a(s)$					
	(exp.)	(b)	(c)	(d)	(e)	(f)
0.00	65.701	66.000	66.000	66.009	66.000	66.009
0.15	57.580	56.665	56.655	56.659	56.644	56.647
0.30	45.203	44.460	44.419	44.413	44.387	44.376
0.45	35.668	35.062	34.980	34.961	34.922	34.895
0.60	27.622	27.348	27.223	27.192	27.142	27.098
0.75	20.785	20.742	20.579	20.538	20.479	20.420
0.90	14.931	15.164	14.970	14.920	14.855	14.784
1.05	10.262	10.633	10.417	10.359	10.292	10.212
1.20	6.653	7.127	6.897	6.835	6.768	6.681
1.35	4.048	4.545	4.313	4.248	4.186	4.095
1.50	2.225	2.735	2.512	2.445	2.391	2.298
1.65	1.058	1.527	1.324	1.257	1.213	1.120
1.80	0.334	0.764	0.589	0.525	0.491	0.402
1.95	−0.065	0.312	0.172	0.112	0.089	0.005
2.10	−0.250	0.067	−0.036	−0.091	−0.102	−0.179
2.25	−0.304	−0.051	−0.119	−0.167	−0.169	−0.236
2.40	−0.293	−0.097	−0.134	−0.174	−0.169	−0.226
2.55	−0.242	−0.105	−0.120	−0.151	−0.140	−0.186
2.70	−0.185	−0.096	−0.096	−0.118	−0.105	−0.138
2.85	−0.124	−0.081	−0.072	−0.086	−0.073	−0.094
3.00	−0.083	−0.066	−0.053	−0.060	−0.049	−0.060
3.15	−0.045	−0.053	−0.039	−0.040	−0.032	−0.035
3.30	−0.028	−0.042	−0.029	−0.026	−0.022	−0.019
3.45	−0.011	−0.033	−0.022	−0.017	−0.016	−0.009
3.60	0.000	−0.026	−0.017	−0.011	−0.012	−0.004
3.75	0.003	−0.020	−0.014	−0.008	−0.009	−0.002
3.90	0.008	−0.015	−0.011	−0.006	−0.007	−0.001
4.05	0.008	−0.012	−0.008	−0.005	−0.006	−0.001
4.20	0.005	−0.009	−0.006	−0.004	−0.005	−0.001
4.35	0.003	−0.006	−0.004	−0.003	−0.003	−0.001
4.50	−0.004	−0.005	−0.003	−0.002	−0.002	0.000
4.65	−0.002	−0.003	−0.002	−0.001	−0.001	0.000
4.80	−0.002	−0.002	−0.001	−0.001	−0.001	0.000

kg m/s). After the Fourier analysis to $B^a(s)$, the convolution of $J^c(q)$ therefore leads to a different multiplicative attenuation of the reciprocal form factor $B(s)$ to $B^a(s)$. Hence, the attenuation of the powder data has subsequently been changed to the value of the single-crystal ones to put all data on the same footing. For the same reason, all theoretical reciprocal form factors $B(s)$ had to be multiplied with the Gaussian function $G(s) = \exp[-(s/3.2514\ \text{Å})^2]$ for the comparison.

3. Quantum-Mechanical Calculations

The calculations were done by using the density functional LCAO-MO-SCF program of Baerends et al. [11] with a triple-zeta basis set [7] of Cartesian Slater-type orbitals (STOs) with polarisation functions up to 3d for the hydrogen atoms and up to 4f for carbon (frozen 1s-core) and oxygen (frozen 1s-core) atoms. The frozen-core approximation [12] on C and O saved computer time and disk storage capacity without reducing the quality of the calculated wave functions significantly. The applied exchange-correlation (XC) potential was a sum of the local approximation to exchange owing to Kohn and Sham [13] and the local approximation to correlation of Vosko, Wilk and Nusair (VWN) [14], which is based on Monte-Carlo studies of Ceperly and Alder [15] for the homogeneous electron gas. The exchange-correlation potential was modified with the method of Stoll [16, 17] to correct the overestimation of the correlation between electrons with the same spin in the local density approximation (LDA). The cluster calculations (Fig. 2a, c) were corrected for the basis set superposition error (BSSE) according to Boys and Bernardi's counterpoise principle [18] by evaluating the fragments of the complex in the combined basis set of the whole complex.

The different clusters (Fig. 2a–d) were built up from fragment molecules (procomplex). The advantages of this method are the transparent analysis of the weak interactions in a cluster and a good starting point for the LDA-SCF iteration of the complex. Our symmetrical-orthogonalisation program is based on a series expansion according to Löwdin [19, 20]. The directional reciprocal form factors were obtained by autocorrelation of the one-electron wave functions in position space. The isotropic $B^a(s)$ was calculated by Fourier transformation of the spherically averaged momentum density.

The theoretical analysis of the reciprocal form factor in the direction of the hydrogen bonds of α-oxalic acid dihydrate is based on the comparison between LDA-SCF and symmetrical-orthogonalisation results for the donor-acceptor system in a fixed geometry. The scheme of thus decomposing $B(s)$ into first-order (symmetrical orthogonalisation) and higher-order (LDA-SCF) effects [1] is analogous to an analysis of the interaction energy in terms of various energy contributions [21].

4. Results and Discussion

The $B^a(s)$-curves for the comparison of theory and experiment (Fig. 3a–e) are drawn in the s-range from

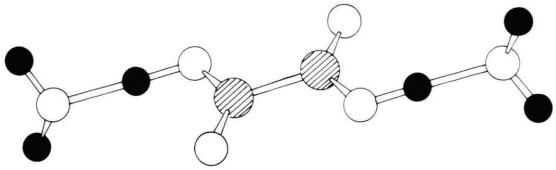

Fig. 2a. Cluster A: $C_2H_2O_4 \cdot 2H_2O$. The molecules were drawn by using shaded circles for carbon, filled circles for hydrogen and empty circles for the oxygen atoms in the Figures 2a–d.

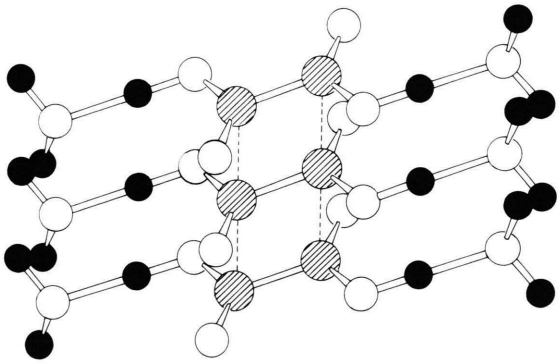

Fig. 2b. Cluster B: $(C_2H_2O_4 \cdot 2H_2O)_3$.

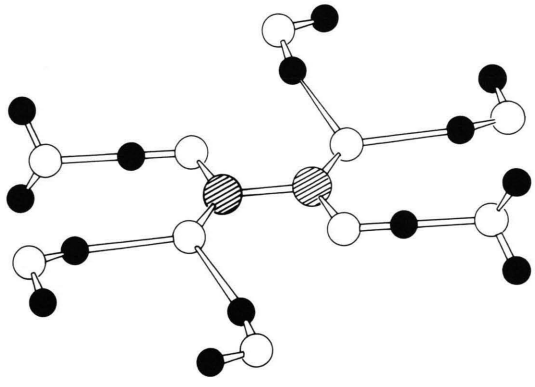

Fig. 2c. Cluster C: $(C_2H_2O_4 \cdot 2H_2O) \cdot 4H_2O$.

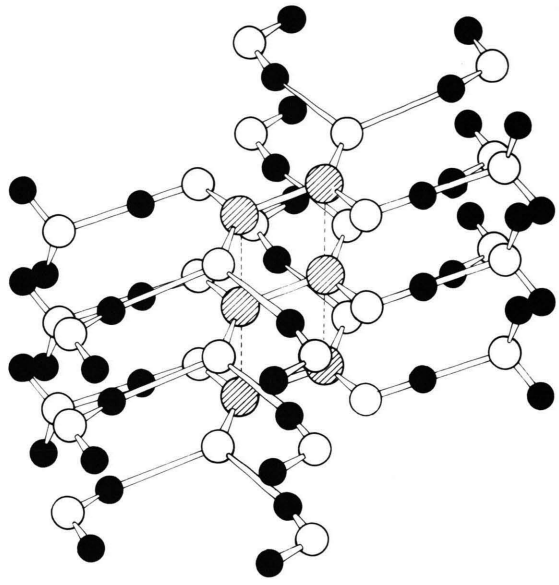

Fig. 2d. Cluster D: $[(C_2H_2O_4 \cdot 2H_2O) \cdot 4H_2O]_3$.

1.2 to 5.0 Å. The orbital contributions of the 1s core electrons of oxygen and carbon virtually vanish beyond 1.5 Å, so that all these curves are dominated by the valence electrons.

The measured reciprocal form factor of α-$(COOH)_2 \cdot 2H_2O$ is necessarily a superposition of two different interaction components in the crystal structure, since the almost planar oxalic-acid molecules of neighbouring stacks are tilted against each other. This fact reduces the anisotropy of the momentum density of α-oxalic acid dihydrate in most directions, but not in the (***a***, ***c***)-plane and parallel to the ***b***-direction (Fig. 3b).

The difference of the experimental and the theoretical data depends strongly on the selected direction in the crystal (see Fig. 3a, b, d) and on the corresponding cluster type (Figure 2a–d). The oxalic-acid molecules in the crystal are influenced by hydrogen bonds and weak intermolecular interactions of the neighbouring molecules. The $[(C_2H_2O_4 \cdot 2H_2O) \cdot 4H_2O]_3$ cluster (cluster D) calculation generally shows the best agreement between theory and experiment (see curve (f), Fig. 3a–e), because all first-order interaction contributions of the first coordination sphere are included by symmetrical orthogonalisation (Figure 2d). The reduced anisotropy of the experimental reciprocal form factor is the result of a superposition of different intermolecular interactions and necessitates to compare the experimental data with the results of calculations for large clusters in order to obtain a better agreement (see, e.g., Figure 3c, d).

The small deviation of the curves (e) and (f) in Fig. 3b shows that the ***b***-direction is dominated by the stack of oxalic-acid and water molecules (see Fig. 2b) in the crystal structure. The hydrogen bonds are located in the plane of the oxalic-acid molecule, perpendicular to the selected orientation of the scattering vector parallel to ***b*** in the measurement (see Figure 1).

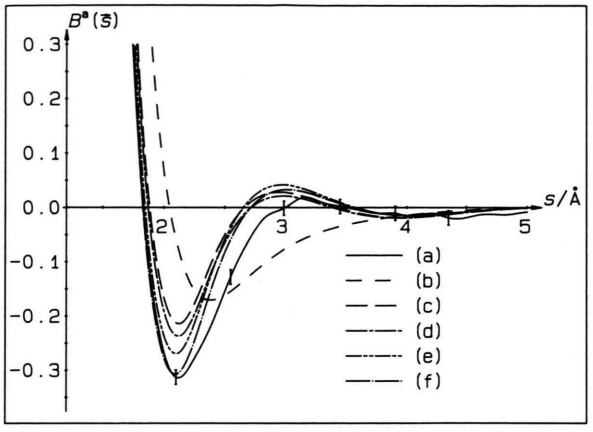

Fig. 3a. $B^a(s)$ in the direction of the strongest hydrogen bond (see I in Fig. 1) as a function of s, theory vs. experiment. (a) The experimental reciprocal form factor $B^a(s)$. (b) The $B^a(s)$-curve resulting from a superposition of the contributions from one oxalic-acid molecule and one pair of water molecules (cluster A). (c) The $B^a(s)$-curve of an LDA-calculation of the oxalic acid dihydrate complex (cluster A). (d) The $B^a(s)$-curve is the result from a symmetrical-orthogonalisation procedure of three LDA wave functions of the oxalic acid dihydrate complex (cluster B). (e) The $B^a(s)$-curve of a symmetrical-orthogonalisation calculation of the α-$(COOH)_2 \cdot 2H_2O$ LDA wave function including the first-order interactions of the four nearest water molecules (cluster C). (f) The $B^a(s)$-curve resulting from a symmetrical-orthogonalisation procedure of the α-$(COOH)_2 \cdot 2H_2O$ LDA wave function in the neighbourhood of the complete first coordination-sphere (cluster D).

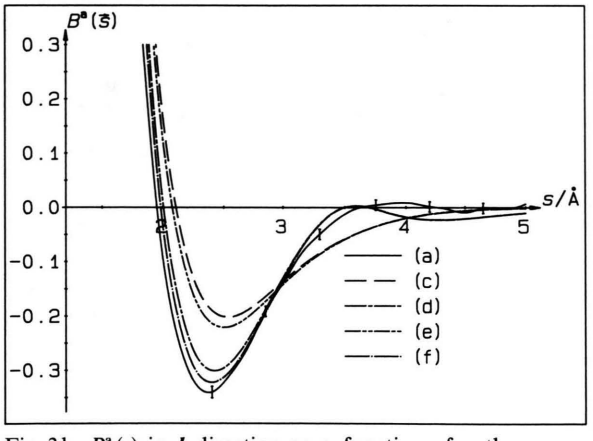

Fig. 3b. $B^a(s)$ in ***b***-direction as a function of s, theory vs. experiment (curves (a)–(f) analogous to Figure 3a).

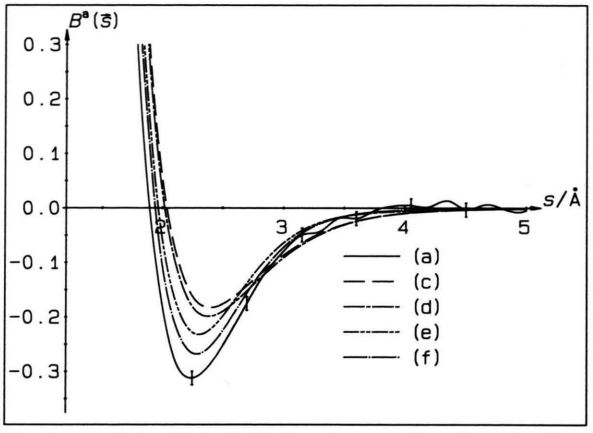

Fig. 3c. $B^a(s)$ in C(1)–O(1) direction as a function of s, theory vs. experiment (curves (a)–(f) analogous to Figure 3a).

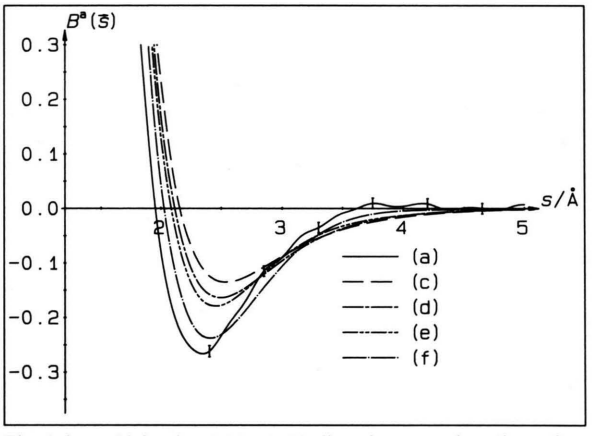

Fig. 3d. $B^a(s)$ in the C(1)–O(2) direction as a function of s, theory vs. experiment (curves (a)–(f) analogous to Figure 3a).

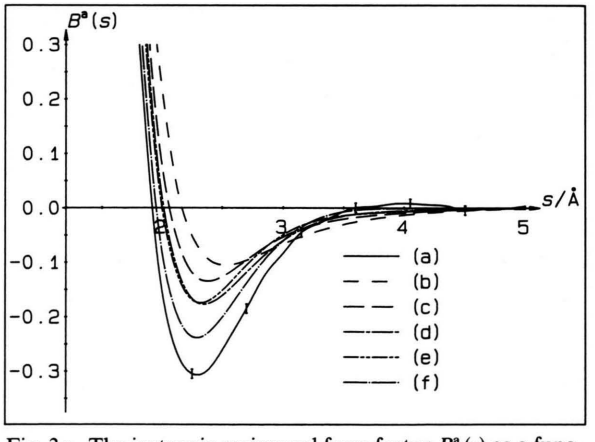

Fig. 3e. The isotropic reciprocal form factor $B^a(s)$ as a function of s, theory vs. experiment (curves (a)–(f) analogous to Figure 3a). A summary of the experimental and theoretical data is given in Table 1.

Table 2. Theoretical analysis of the O(3)–H(1) hydrogen bond.

s/Å	$B(s)$				
	LDA tot.*	LDA ort.§	LDA sup.§	HF tot.*	HF sup.§
0.00	66.0000	66.0000	66.0000	66.0000	66.0000
0.15	56.7440	56.7206	56.7646	56.7077	56.7337
0.30	44.7026	44.6320	44.7774	44.6563	44.7483
0.45	35.5049	35.3806	35.6488	35.4140	35.5867
0.60	27.9850	27.8067	28.2012	27.7532	28.0064
0.75	21.5031	21.2780	21.7930	21.0965	21.4283
0.90	15.9138	15.6592	16.2816	15.3581	15.7696
1.05	11.2054	10.9509	11.6585	10.5617	11.0550
1.20	7.3887	7.1749	7.9344	6.7340	7.3079
1.35	4.4502	4.3159	5.0865	3.8520	4.4949
1.50	2.3335	2.2924	3.0351	1.8305	2.5102
1.65	0.9221	0.9559	1.6353	0.5274	1.1895
1.80	0.0734	0.1490	0.7234	−0.2183	0.3583
1.95	−0.3319	−0.2507	0.1663	−0.5396	−0.1212
2.10	−0.3999	−0.3471	−0.1425	−0.5517	−0.3578
2.25	−0.2494	−0.2509	−0.2859	−0.3743	−0.4371
2.40	−0.0367	−0.1014	−0.3275	−0.1471	−0.4251
2.55	0.1013	−0.0131	−0.3182	0.0157	−0.3712
2.70	0.1533	0.0166	−0.2949	0.1001	−0.3084
2.85	0.1490	0.0151	−0.2698	0.1249	−0.2492
3.00	0.1080	−0.0066	−0.2451	0.1069	−0.1981
3.15	0.0442	−0.0420	−0.2228	0.0618	−0.1580
3.30	−0.0288	−0.0833	−0.2040	0.0042	−0.1291
3.45	−0.0992	−0.1227	−0.1883	−0.0533	−0.1097
3.60	−0.1579	−0.1538	−0.1743	−0.1017	−0.0972
3.75	−0.1992	−0.1725	−0.1604	−0.1360	−0.0883
3.90	−0.2205	−0.1772	−0.1452	−0.1549	−0.0804
4.05	−0.2227	−0.1687	−0.1283	−0.1594	−0.0720
4.20	−0.2091	−0.1502	−0.1105	−0.1519	−0.0627
4.35	−0.1838	−0.1254	−0.0925	−0.1356	−0.0529
4.50	−0.1515	−0.0985	−0.0754	−0.1137	−0.0434
4.65	−0.1160	−0.0728	−0.0597	−0.0892	−0.0345
4.80	−0.0809	−0.0509	−0.0456	−0.0647	−0.0267
4.95	−0.0490	−0.0335	−0.0333	−0.0426	−0.0200
5.10	−0.0238	−0.0202	−0.0229	−0.0250	−0.0146
5.25	−0.0075	−0.0106	−0.0144	−0.0129	−0.0103
5.40	0.0006	−0.0049	−0.0078	−0.0054	−0.0069
5.55	0.0033	−0.0021	−0.0027	−0.0013	−0.0044
5.70	0.0038	−0.0005	0.0011	0.0007	−0.0025
5.85	0.0037	0.0006	0.0039	0.0014	−0.0013
6.00	0.0038	0.0016	0.0061	0.0015	−0.0005

* Calculation of the complete complex. § Symmetrical-orthogonalisation. § Procomplex without interaction.

Table 3. Theoretical analysis of the O(2)–H(2) hydrogen bond with LDA.

s/Å	$B(s)$		
	LDA tot.*	LDA ort.§	LDA sup.§
0.00	82.0000	82.0000	82.0000
0.15	77.7623	77.7437	77.7675
0.30	68.5459	68.4892	68.5671
0.45	57.7798	57.6786	57.8221
0.60	46.9588	46.8115	47.0231
0.75	36.7959	36.6045	36.8827
0.90	27.6932	27.4639	27.8050
1.05	19.9273	19.6715	20.0700
1.20	13.6669	13.4009	13.8487
1.35	8.8991	8.6430	9.1290
1.50	5.4253	5.2012	5.7099
1.65	2.9823	2.8110	3.3219
1.80	1.3337	1.2291	1.7172
1.95	0.2864	0.2479	0.6884
2.10	−0.3132	−0.3023	0.0680
2.25	−0.5860	−0.5502	−0.2749
2.40	−0.6285	−0.5930	−0.4377
2.55	−0.5253	−0.5110	−0.4906
2.70	−0.3615	−0.3802	−0.4814
2.85	−0.2136	−0.2636	−0.4407
3.00	−0.1145	−0.1845	−0.3871
3.15	−0.0584	−0.1351	−0.3310
3.30	−0.0328	−0.1057	−0.2777
3.45	−0.0276	−0.0902	−0.2298
3.60	−0.0352	−0.0834	−0.1885
3.75	−0.0491	−0.0815	−0.1541
3.90	−0.0641	−0.0815	−0.1262
4.05	−0.0769	−0.0812	−0.1041
4.20	−0.0854	−0.0796	−0.0869
4.35	−0.0888	−0.0762	−0.0736
4.50	−0.0874	−0.0710	−0.0633
4.65	−0.0820	−0.0645	−0.0551
4.80	−0.0737	−0.0570	−0.0484
4.95	−0.0639	−0.0492	−0.0427
5.10	−0.0535	−0.0416	−0.0378
5.25	−0.0433	−0.0344	−0.0334
5.40	−0.0340	−0.0280	−0.0295
5.55	−0.0259	−0.0224	−0.0259
5.70	−0.0192	−0.0178	−0.0227
5.85	−0.0138	−0.0140	−0.0198
6.00	−0.0097	−0.0111	−0.0173

* Calculation of the complete complex. § Symmetrical-orthogonalisation. § Procomplex without interaction.

The influence of hydrogen bonding on the reciprocal form factor is revealed in Fig. 3 a by comparing the various cluster models. The high sensitivity of $B^a(s)$ for intermolecular interactions is indicated by the large difference of the curves (b), (c), and (f) in Figure 3 a. The weak hydrogen bonds (see curves (c) and (e) in Fig. 3 a) also influence the data since the O(2)···H(3) bond is nearly parallel to the direction of the strongest hydrogen bond (III and I in Fig. 1). The oscillating behaviour of the data can be attributed to the association of the water and acid molecules in the crystal (compare (b) and (c) in Figure 3 a).

The influence of the second weak hydrogen bond (II in Fig. 1) can be seen in Fig. 3 c (see curve (c), (e)). The situation is similar to that of Fig. 3 a, because the C(1)–O(1) orientation of the scattering vector points into almost the same direction as the second weak hydrogen bond of the proton-acceptor oxygen O(2).

The theoretical analysis of the three different hydrogen bonds in $B^a(s)$ is based on the attenuated differ-

Table 4. Theoretical analysis of the O(2)–H(3) hydrogen bond with LDA.

s/Å	B(s)		
	LDA tot.*	LDA ort.§	LDA sup.§
0.00	82.0000	82.0000	82.0000
0.15	77.6558	77.6366	77.6604
0.30	68.1937	68.1350	68.2131
0.45	57.1733	57.0697	57.2131
0.60	46.1888	46.0399	46.2507
0.75	36.0006	35.8099	36.0858
0.90	26.9941	26.7693	27.1057
1.05	19.3611	19.1147	19.5052
1.20	13.1681	12.9174	13.3535
1.35	8.3734	8.1395	8.6098
1.50	4.8486	4.6531	5.1423
1.65	2.4038	2.2658	2.7534
1.80	0.8297	0.7612	1.2219
1.95	−0.0653	−0.0651	0.3428
2.10	−0.4511	−0.3991	−0.0660
2.25	−0.4873	−0.4096	−0.1715
2.40	−0.3280	−0.2509	−0.1255
2.55	−0.1054	−0.0499	−0.0455
2.70	0.0884	0.1105	0.0099
2.85	0.2059	0.1939	0.0235
3.00	0.2408	0.2024	0.0049
3.15	0.2140	0.1605	−0.0312
3.30	0.1519	0.0940	−0.0720
3.45	0.0755	0.0220	−0.1089
3.60	−0.0008	−0.0434	−0.1372
3.75	−0.0684	−0.0957	−0.1553
3.90	−0.1221	−0.1321	−0.1635
4.05	−0.1598	−0.1526	−0.1632
4.20	−0.1811	−0.1589	−0.1564
4.35	−0.1869	−0.1536	−0.1448
4.50	−0.1791	−0.1397	−0.1303
4.65	−0.1603	−0.1200	−0.1142
4.80	−0.1335	−0.0974	−0.0977
4.95	−0.1023	−0.0740	−0.0815
5.10	−0.0703	−0.0520	−0.0664
5.25	−0.0416	−0.0333	−0.0528
5.40	−0.0197	−0.0195	−0.0409
5.55	−0.0055	−0.0107	−0.0309
5.70	0.0025	−0.0054	−0.0224
5.85	0.0064	−0.0023	−0.0153
6.00	0.0079	−0.0003	−0.0095

* Calculation of the complete complex. § Symmetrical-orthogonalisation. § Procomplex without interaction.

Table 5. Comparison of Hartree-Fock and LDA for the Ne atom.

s/Å	$B^a(s)$		
	HF	HFS	LDA
0.00	10.0000	10.0000	10.0000
0.15	8.0260	7.9934	7.9993
0.30	5.8004	5.8322	5.8443
0.45	4.1082	4.1621	4.1781
0.60	2.7870	2.8391	2.8562
0.75	1.8020	1.8567	1.8726
0.90	1.1097	1.1616	1.1749
1.05	0.6481	0.6887	0.6989
1.20	0.3547	0.3800	0.3873
1.35	0.1769	0.1879	0.1927
1.50	0.0744	0.0748	0.0778
1.65	0.0191	0.0130	0.0147
1.80	−0.0082	−0.0173	−0.0165
1.95	−0.0194	−0.0293	−0.0291
2.10	−0.0222	−0.0315	−0.0316
2.25	−0.0208	−0.0288	−0.0291
2.40	−0.0177	−0.0243	−0.0247
2.55	−0.0142	−0.0195	−0.0198
2.70	−0.0110	−0.0151	−0.0154
2.85	−0.0083	−0.0114	−0.0116
3.00	−0.0061	−0.0084	−0.0086
3.15	−0.0044	−0.0061	−0.0062
3.30	−0.0031	−0.0043	−0.0044
3.45	−0.0022	−0.0030	−0.0031
3.60	−0.0015	−0.0021	−0.0022
3.75	−0.0010	−0.0015	−0.0015
3.90	−0.0007	−0.0010	−0.0010
4.05	−0.0005	−0.0007	−0.0007
4.20	−0.0003	−0.0005	−0.0005
4.35	−0.0002	−0.0003	−0.0003
4.50	−0.0001	−0.0002	−0.0002
4.65	−0.0001	−0.0001	−0.0001
4.80	−0.0001	−0.0001	−0.0001

ence of LDA and symmetrical-orthogonalisation calculations (see Tables 2–4) for the corresponding hydrogen-bonded clusters (Figure 2a, c). The curves indicate that in the higher-*s*-value region (Fig. 4b, c), which was considered for the comparison with the experimental data, it is a good approximation to take into account the influence of the weak hydrogen bonds by symmetrical orthogonalisation. The neglect of higher-order effects led, however, to an overestimation of the association effect in the low-*s*-value range (Figures 4a–c).

The accuracy of density functional calculations is limited by the approximation made for the exchange-correlation potential term. The comparison of the reciprocal form factors that were calculated with the Hartree-Fock-Slater (HFS) [22, 23] and the LDA method indicated only a small effect of the density functional on the autocorrelation of wave functions in position space. The correction for electron-electron correlation in the spin-restricted case [16, 17], on the other hand, provided the main contribution to the difference between both calculation procedures. Krijn obtained similar results in the electron density distribution of CO and H_2O molecules [24].

The calculation of our theoretical data is based on autocorrelation of LDA-orbitals (approximate Kohn-Sham orbitals) in position space. This procedure is customarily employed, but only correct for Hartree-Fock wave functions. Lam and Platzman [25, 26]

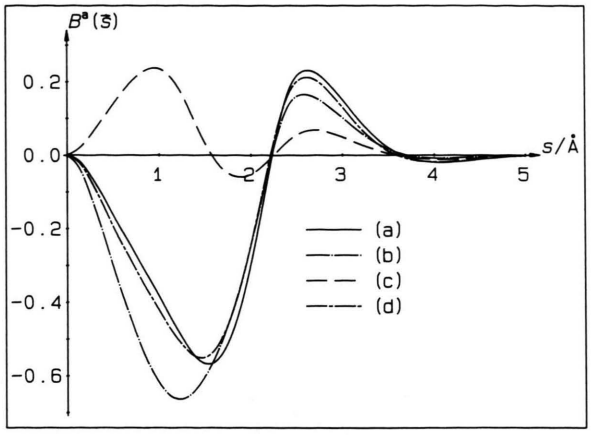

Fig. 4a. A theoretical analysis of $B^a(s)$ in the direction of the strongest hydrogen bond O(3)···H(1). In contrast to the calculated reciprocal form factors that were compared with the experimental data, the $B^a(s)$ curves for the hydrogen-bond analysis are not the average for a tilted pair of α-$(COOH)_2 \cdot 2H_2O$ units; the curves rather hold for a single unit with s parallel to the shortest hydrogen bond (I). (a) The $B^a(s)$ of the total interaction of the donor-acceptor system calculated with the LDA method. (b) The $B^a(s)$ of the first-order terms (electrostatic and exchange interaction). (c) The $B^a(s)$ of the higher-order terms (polarisation and charge transfer). (d) The $B^a(s)$ of the total interaction of the donor-acceptor system determined by a Hartree-Fock calculation with an extended Gaussian double-zeta basis set (cf. curve (a)).

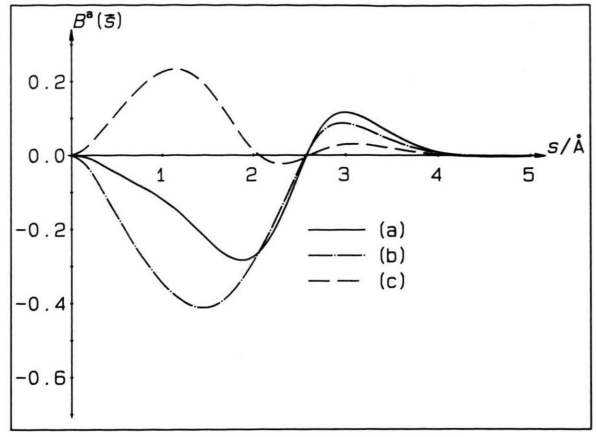

Fig. 4b. A theoretical analysis of $B^a(s)$ in the direction of the weak hydrogen bond O(2)···H(2) (II) (curves (a)–(c) analogous to Figure 4a).

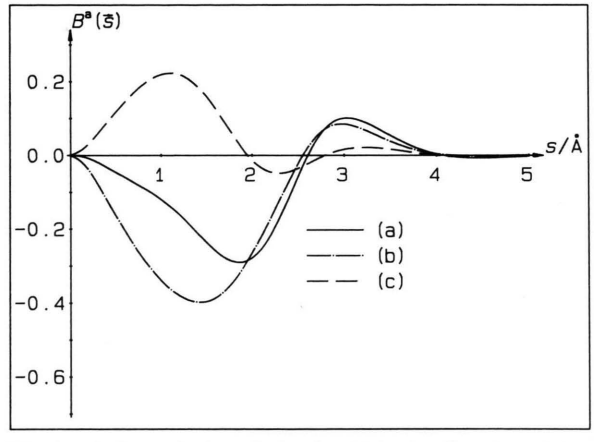

Fig. 4c. A theoretical analysis of $B^a(s)$ in the direction of the longest hydrogen bond O(2)···H(3) (III) (curves (a)–(c) analogous to Figure 4a).

showed by deducing the ground-state momentum density from the Fourier-transformed Kohn-Sham equations [13] that $\pi(\boldsymbol{p})$ is modified by the addition of an extra term that is the derivative of the total exchange-correlation energy with respect to the individual electron energies arising from correlation between the one-electron states. Cardwell and Cooper [27] applied the (isotropic) Lam-Platzman correction [25] to solid-state LDA calculations (core and valence electrons) of Al, Fe, Cr, Ni, and V. We transformed these difference Compton profiles to our attenuated reciprocal form factor in order to get an estimate for the contribution of the correction. The results had a maximum deviation of $-0.11\,e^-$ in the case of aluminium ($Z = 13$) and $-0.105\,e^-$ in the case of iron ($Z = 26$) in the low-s-value region. The deviation decreases rapidly above $s = 1.5$ Å. The subtraction of $B^a(s)$ of Hartree-Fock and LDA calculations (within the same STO basis set) of Ne [28] and CO [29] led to results of the same order of magnitude (see Tables 5, 6).

An ab-initio SCF Hartree-Fock (HF) calculation for the α-oxalic acid dihydrate complex was performed ($E_{tot} = -528.5501\,E_h$) with the program GAMESS [30] using a Gaussian double-zeta basis set [31] augmented with 3d polarisation functions for carbon (exponent $\alpha = 0.7$) and oxygen ($\alpha = 0.9$) and 2p for hydrogen ($\alpha = 0.9$) and was corrected for the BSSE [18] (interaction energy $0.0208\,E_h$). For the analysis of the intermolecular interactions in the direction of the shortest hydrogen bond, the difference in $B^a(s)$ between the complex and its constituents (procomplex) was calculated with each theoretical method (LDA and HF). We have found a remarkably good agreement between both difference curves over the whole range of s-values (see curve (a) and (d) in Figure 4a). Also when taking the average of a pair of complexes tilted as in the crystal, the HF data (not shown in Fig. 3a) in the direction of that shortest hydrogen

Table 6. Comparison of HF and LDA for a CO molecule in x (column 2 and 3) and z direction (column 4 and 5).

s/Å	$B^a(s)$			
	HF	LDA	HF	LDA
0.00	10.0000	10.0000	10.0000	10.0000
0.15	9.4677	9.4557	9.4724	9.4653
0.30	8.3006	8.2728	8.3282	8.3180
0.45	6.9361	6.9055	7.0020	7.0061
0.60	5.5843	5.5651	5.6794	5.7112
0.75	4.3547	4.3544	4.4503	4.5114
0.90	3.3011	3.3200	3.3833	3.4656
1.05	2.4400	2.4737	2.5441	2.6373
1.20	1.7631	1.8060	1.9359	2.0344
1.35	1.2483	1.2951	1.4799	1.5780
1.50	0.8679	0.9143	1.1250	1.2159
1.65	0.5937	0.6368	0.8494	0.9289
1.80	0.4003	0.4386	0.6392	0.7062
1.95	0.2664	0.2992	0.4818	0.5368
2.10	0.1753	0.2027	0.3650	0.4096
2.25	0.1143	0.1366	0.2783	0.3141
2.40	0.0740	0.0919	0.2135	0.2421
2.55	0.0477	0.0618	0.1645	0.1871
2.70	0.0307	0.0416	0.1269	0.1447
2.85	0.0198	0.0282	0.0977	0.1117
3.00	0.0128	0.0192	0.0749	0.0858
3.15	0.0084	0.0132	0.0571	0.0656
3.30	0.0055	0.0091	0.0432	0.0497
3.45	0.0037	0.0064	0.0325	0.0373
3.60	0.0025	0.0045	0.0241	0.0278
3.75	0.0018	0.0032	0.0178	0.0205
3.90	0.0012	0.0023	0.0130	0.0150
4.05	0.0009	0.0016	0.0094	0.0109
4.20	0.0006	0.0012	0.0067	0.0078
4.35	0.0005	0.0008	0.0048	0.0055
4.50	0.0003	0.0006	0.0033	0.0039
4.65	0.0002	0.0004	0.0023	0.0027
4.80	0.0002	0.0003	0.0016	0.0019

bond (I in Fig. 1) show the same oscillating behaviour of the reciprocal form factor as the LDA results (compare curves (b) and (c) in Figure 3a). On the other hand, the first zero-passage of the $B^a(s)$ curves in the HF approximation is in most of the directions closer to the experiment than in the LDA case. That deviation of the LDA with respect to the HF results must be due to the different quantum-mechanical ansatz of both methods and the two different types and sizes of basis sets used in our calculation.

5. Conclusion

The comparison of the experimental and the theoretical data has demonstrated that the reciprocal form factor is far more sensitive to intermolecular interactions in the solid state than the corresponding electron-density data [7].

In our theoretical calculations we have introduced the intermolecular interactions of the α-$(COOH)_2 \cdot 2H_2O$ unit by a cluster of increasing size. The main advantage of cluster calculations is the possibility to discuss the effect of the crystal environment in molecular and hence chemical terms.

Calculations that include the first coordination shell of the oxalic-acid molecule in the crystal have turned out to be a good approximation to the electronic structure of the crystal in the direction of the strongest hydrogen bond and in the ***b***-direction. The poorer agreement between the experimental and theoretical data in the direction of the C = O and C – O bonds, on the other hand, indicates that also the second coordination shell – consisting of the neighbouring oxalic-acid molecules – contributes significantly to the intermolecular interactions in those directions. For the C = O bond it is the O = C bond of the next oxalic-acid molecule, linked by a pair of water molecules in a puckered eight-membered ring, that is not taken into account in the cluster calculation, while the oxygen O(1) of the C – O bond "sees" another oxygen atom of the same type of an oxalic-acid molecule of the tilted chain in the crystal at a distance of 3.196 Å close to the extrapolated bond axis, again not included in the cluster.

For the three hydrogen bonds, we can further conclude from our $B^a(s)$-curves (Fig. 4a–c) that the long-range interactions (high-s-value region) are dominated by first-order effects, whereas in the short-range interactions (small-s-values) also higher-order effects play an important rôle. This corroborates our earlier findings for the hydrogen bonds in $KHCO_3$ [1].

Finally, we have found that the absolute $B^a(s)$ values obtained from our LDA and HF calculations deviate from each other. The intermolecular interactions as seen in the difference curves $\Delta B^a(s)$ (cluster minus constituents), however, are in good agreement and thus do not depend on the different ansatzes of both methods (see Figure 4a).

Acknowledgements

The LDA calculations were carried out at the HLRZ in the KFA Jülich, Germany. We wish to thank Prof. Dr. E. J. Baerends for supplying us with a new version of his LDA program package and Dr. P. Vernooijs for his very valuable help to adapt the Fortran source code to VAX and Cray computers. We are furthermore very grateful to the Fonds der Chemischen Industrie for its continuous financial support.

[1] M. Bräuchler, S. Lunell, I. Olovsson, and W. Weyrich, Int. J. Quantum Chem. **35,** 895 (1989).
[2] B. Williams, Ed., Compton Scattering. The Investigation of Electron Momentum Distributions, McGraw-Hill, New York 1977.
[3] M. J. Cooper, Rep. Prog. Phys. **48,** 415 (1985).
[4] P. Coppens (Project Reporter), Acta Cryst. **A 40,** 184 (1984).
[5] T. F. Koetzle and R. K. McMullan, Oxalic Acid Project Circular (1980).
[6] M. P. C. M. Krijn, H. Graafsma, and D. Feil, Acta Cryst. **B 44,** 609 (1988).
[7] M. P. C. M. Krijn, J. Chem. Phys. **89,** 4199 (1988).
[8] J. L. Torgesen, J. Strassburger, Science **146,** 53 (1964).
[9] W. Weyrich, Ber. Bunsenges. Phys. Chem. **79,** 1085 (1975).
[10] N. Gérard, G. Watelle-Marion, and A. Thrierr-Sorel, Bull. Soc. Chim. France **5,** 1788 (1967).
[11] E. J. Baerends and P. Ros, Int. J. Quantum Chem. Quantum Chem Symp. **12,** 169 (1978).
[12] E. J. Baerends, D. E. Ellis, and P. Ros, Chem. Phys. **2,** 41 (1973).
[13] W. Kohn and L. J. Sham, Phys. Rev. A **140,** 1133 (1965).
[14] S. H. Vosko, L. Wilk, and M. Nusair, Can. J. Phys. **58,** 1200 (1980).
[15] D. M. Ceperly and B. J. Alder, Phys. Rev. Lett. **45,** 566 (1980).
[16] H. Stoll, C. M. E. Pavlidou, and H. Preuß, Theor. Chim. Acta **149,** 143 (1978).
[17] H. Stoll, E. Golka, and H. Preuß, Theor. Chim. Acta **55,** 29 (1980).
[18] S. F. Boys and F. Bernardi, Mol. Phys. **19,** 553 (1970).
[19] P.-O. Löwdin, Phys. Rev. **97,** 1474 (1955).
[20] P.-O. Löwdin, Adv. Phys. **5,** 1 (1956).
[21] K. Morokuma and K. Kitaura, in: H. Ratajczak and W. J. Orville-Thomas (Eds.), Molecular Interactions, John Wiley & Sons, Chichester etc., 1980, Vol. 1, p. 24.
[22] E. J. Baerends and P. Ros, Chem. Phys. **2,** 52 (1973).
[23] E. J. Baerends and P. Ros, Chem. Phys. **8,** 412 (1975).
[24] M. P. C. M. Krijn and D. Feil, Chem. Phys. Letters **150,** 45 (1988).
[25] L. Lam and P. M. Platzman, Phys. Rev. **9,** 5122 (1974).
[26] L. Lam and P. M. Platzman, Phys. Rev. **9,** 5128 (1974).
[27] D. A. Cardwell and M. J. Cooper, J. Phys.: Cond. Matter **1,** 9357 (1989).
[28] E. Clementi and C. Roetti, At. Data Nucl. Data Tables **14,** 177 (1974).
[29] A. D. McLean and M. Yoshimine, Tables of Linear Molecule Wavefunctions, IBM, New York 1967.
[30] M. W. Schmidt, J. A. Boatz, K. K. Baldridge, S. Koseki, M. S. Gordon, S. T. Elbert, and B. Lam, QCPE Bulletin, Vol. 7, 115, 1987.
[31] T. H. Dunning, Jr., and P. J. Hay, Chapter 1 in H. F. Schaefer III (Ed.), Methods of Electronic Structure Theory, Plenum Press, N.Y. 1977, p. 1–27 (outer scale factor 1.2 changed to 1.15 for hydrogen).